JACS
JOURNAL OF THE AMERICAN CHEMICAL SOCIETY
Article
pubs.acs.org/JACS

Modeling Dioxygen Reduction at Multicopper Oxidase Cathodes

Peter Agbo, James R. Heath, and Harry B. Gray*

Beckman Institute, Noyes Laboratory of Chemical Physics, California Institute of Technology, Pasadena, California 91125, United States

Supporting Information

ABSTRACT: We report a general kinetics model for catalytic dioxygen reduction on multicopper oxidase (MCO) cathodes. Our rate equation combines Butler–Volmer (BV) electrode kinetics and the Michaelis–Menten (MM) formalism for enzymatic catalysis, with the BV model accounting for interfacial electron transfer (ET) between the electrode surface and the MCO type 1 copper site. Extending the principles of MM kinetics to this system produced an analytical expression incorporating the effects of subsequent intramolecular ET and dioxygen binding to the trinuclear copper cluster into the cumulative model. We employed experimental electrochemical data on *Thermus thermophilus* laccase as benchmarks to validate our model, which we suggest will aid in the design of more efficient MCO cathodes. In addition, we demonstrate the model's utility in determining estimates for both the electronic coupling and average distance between the laccase type-1 active site and the cathode substrate.

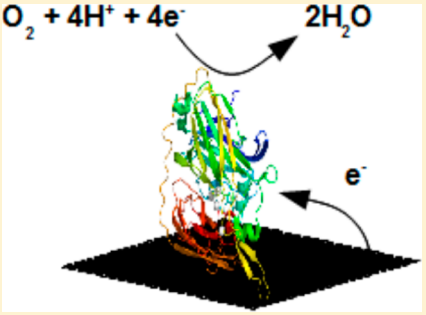

INTRODUCTION

Multicopper oxidases (MCOs) have shown great promise as cathode catalysts in bioinorganic fuel cells.[1−7] It is known that dioxygen reduction in these enzymes proceeds through initial electron transfer (ET) to all metal ions in the resting enzyme, resulting in an all-cuprous (reduced) state (Figure 1, A → B). In the reaction mechanism, diffusion of O_2 into the reduced enzyme, followed by two-electron reduction of the adduct, results in formation of a peroxy intermediate (Figure 1, B → C). Reduction of this adduct by two more electrons affords the "native intermediate" (Figure 1, C → D), which is converted back to the all-cuprous state to close the catalytic cycle. Return to the resting enzyme has been found not to be relevant to the catalytic cycle under steady-state conditions (Figure 1, D → A).[8−12]

In the MCO reaction cycle, outer-sphere oxidation of a donor species by the type 1 site is the rate-limiting step.[8,13] In systems where these proteins have a soluble reductant replaced with a cathodic surface, kinetics are dictated by interfacial charge transfer at lower overpotentials and by O_2 availability at higher driving forces.[1,5,14−20] Despite an extensive body of work on MCO chemistry delineating both the electrochemical behavior of various laccase isoforms and the overall kinetics scheme common to this enzyme family, a rigorous rate law accounting for the electrokinetics of MCOs when functioning as heterogeneous catalysts has yet to be reported. Kamitaka employed a generalized rate equation to fit bilirubin oxidase electrode kinetics, expressed simply as $r = k_{cat}/(1 + k_{cat}/k_f + k_b/k_f)$, where k_{cat} is the limiting rate constant, k_f is the forward interfacial ET rate constant, and k_b is the reverse interfacial ET rate constant.[18] However, this description, while capable of generating voltammetric curves similar to experimental ones, is insufficient because it omits all other rate constants inherent to the MCO reaction scheme from the rate equation.

We have developed a model of MCO electrode kinetics that sheds light on enzyme behavior when operating as a catalytic cathode. The generally accepted catalytic scheme of MCOs includes four intermediate states, with the possibility of eight rate constants being used to express a corresponding rate law; the general equation used by Kamitaka includes only three.

In our model, interfacial charge transfer is expressed using a Butler–Volmer (BV) approach, where the current is scaled by an exponential dependence on overpotential.[21,22] We have further generalized the model by expressing the BV-dependent terms in our rate equation as a function of semiclassical ET theory parameters. We have tested our expression describing MCO cathode kinetics using experimental data from extensive investigations of the electrochemistry of *Thermus thermophilus* laccase.

EXPERIMENTAL METHODS

All modeling was done using the Python programming language with *numpy*, *matplotlib*, and *xlrd* libraries. Laccase purification and electrode assembly were performed as previously described.[23] Thermal titrations employed electrode rotation at 4000 rpm in pH 5.0 20 mM sodium acetate. Electrodes with geometric surface areas of 0.25 cm^2 were used. A scan rate of 10 mV s^{-1} between 600 and 200 mV vs Ag|AgCl using a BAS 100 potentiostat was chosen for measurements. Current at 250 mV vs Ag|AgCl was used for back-calculation of the rates for Eyring analysis that allowed estimation of the type 1 Cu reorganization energy. Reductive titrations of laccase were performed in order to determine the solution values for the type 1 redox potential in this protein (Supporting Information).

Received: July 29, 2014
Published: September 4, 2014

   dx.doi.org/10.1021/ja5077519 | J. Am. Chem. Soc. 2014, 136, 13882−13887

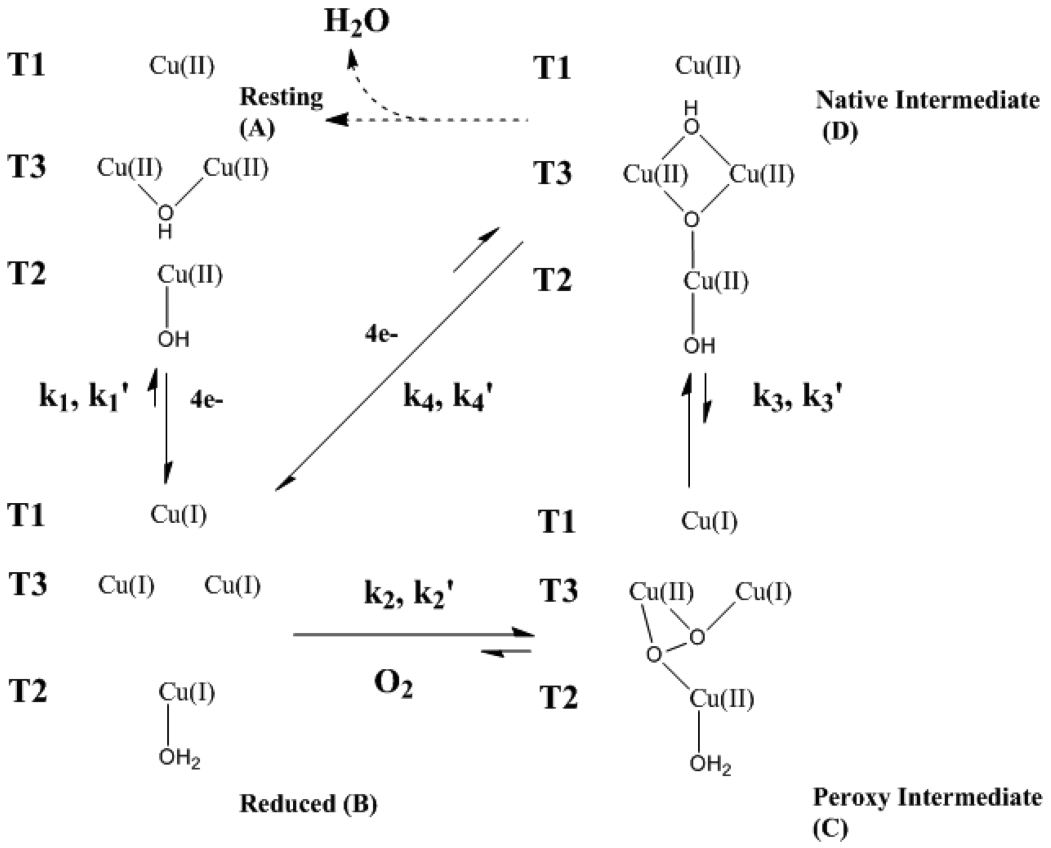

Figure 1. Catalytic cycling of dioxygen reduction to water by a multicopper oxidase. Forward rate constants are denoted k_n, reverse rate constants are of the form k_n'.

RESULTS

Starting with the kinetics scheme common to laccases (Figure 1), we write the overall rate law for dioxygen reduction by *Thermus thermophilus* laccase, where O_2 binding (k_2, k_2') is the limiting step:

$$r = k_2[\mathrm{B}][\mathrm{O}_2] - k_2'[\mathrm{C}] \tag{1}$$

A system of differential equations expressing the changing concentrations of all four intermediates is then assembled, allowing us to express the unknown intermediate concentrations in terms of total enzyme surface concentration, N_T (Supporting Information). Explicit solution for the concentration of all intermediates gives a cathodic rate equation, which, when expressed as a cathodic current density (j), yields:

$$j(\eta) = -\frac{eFk_1N_T(k_2[\mathrm{O}_2] - k_2'f)}{N_AG\left(1 + \frac{k_1}{G}\left(1 + f + \frac{k_3f + k_4'}{k_3' + k_4}\right)\right)} \tag{2}$$

where

$$f = \frac{k_2[\mathrm{O}_2](k_3' + k_4)}{(k_3' + k_4)(k_2' + k_3) - k_3 + k_3'} \tag{3}$$

and

$$G = k_4' + k_1' + k_2[\mathrm{O}_2] - k_2'f - \frac{k_4(k_3f + k_4')}{k_3' + k_4} \tag{4}$$

Dependence of j on the overpotential, η, arises from the rates k_1, k_1', k_4, and k_4'. Terms k_1 and k_4 represent the forward rate constants for interfacial charge transfer, which can be expressed by substituting the exchange rate term of the BV model for the semiclassical (Marcus) equation when $\Delta G^0 = 0$ (Supporting Information):

$$k_1 = k_4 = \frac{4\pi^2}{h\sqrt{4\pi\lambda k_BT}}H_{AB}^2\exp\left(\frac{-\lambda}{4k_BT}\right)\exp\left(\frac{-\alpha nF\eta}{RT}\right) \tag{5}$$

An analogous description for the reverse interfacial rate constants (k_1' and k_4') then follows:

$$k_1' = k_4' = \frac{4\pi^2}{h\sqrt{4\pi\lambda k_BT}}H_{AB}^2\exp\left(\frac{-\lambda}{4k_BT}\right)\exp\left(\frac{(1-\alpha)nF\eta}{RT}\right) \tag{6}$$

In the high overpotential limit, the current density transforms to a function independent of η, reducing eq 2 to

$$j = -\frac{eFN_Tk_2[\mathrm{O}_2]\left(1 - \frac{k_2'}{k_3}\right)}{N_A\left(1 + \frac{k_2[\mathrm{O}_2]}{k_3}\right)} \tag{7}$$

Values used as modeling parameters were taken from studies of laccase on ketjen black electrodes: $N_T = 1.56 \times 10^{14}$ cm^{-2}, F is Faraday's constant (96485 C mol^{-1}), e is the total number of electrons transferred during a single catalytic turnover (4), n is the number of electrons transferred during a single interfacial charge-transfer event (1), λ is the type 1 site reorganization energy, T is temperature (303 K), H_{AB} is the electronic coupling between the type 1 site and the electrode surface, η is the overpotential and α is the symmetry factor (0.48).[23] Rate constants (k_n, k_n') are defined in Figure 1.

dx.doi.org/10.1021/ja5077519 | J. Am. Chem. Soc. 2014, 136, 13882−13887

The reorganization energy for the type 1 center on these electrodes was estimated from the temperature dependence of current production in the low overpotential range, where kinetics are dominated by interfacial ET to the type 1 copper site. From the values of current between 20 and 50 °C at η = −90 mV, we find $\Delta G^{\ddagger}$ =15 kJ mol^{-1} for reduction of type 1 Cu (Figures S.2 and S.3). The type 1 reorganization energy can then be estimated from eq 8:[24]

$$\Delta G^{\ddagger} = (\Delta G + \lambda)^2/4\lambda \quad (8)$$

where ΔG is calculated using the relation $\Delta G = -nF\eta$. Here, analysis of thermal titration data yielded λ = 0.4 eV. Besides falling within the range of literature values for type 1 copper reorganization energies, this estimate is close to that reported for azurin hydrophobically adsorbed to Au-alkanethiol electrodes (0.33 eV).[25] These lower values for type 1 reorganization should be expected for physisorbed blue-copper systems, as hydrophobic binding of the protein will result in exclusion of water at the electrode surface (desolvation will reduce the outer-sphere contribution to the total reorganization energy of the type 1 copper site). With these parameters in hand, we calculate a coupling (H_{AB}) of 6.6 × 10^{-27} J (330 μcm^{-1}) per enzyme (eq 5 or 6).

The reported dependence of the catalytic current on dissolved O_2 concentration indicates that the step B ↔ C controls electrokinetics at limiting values of the current, as the conversion of the reduced enzyme to the peroxy intermediate is the rate-limiting step (the net rate of reaction is as described by eq 1). We have determined the overall rate, r, to be 5 and 6 s^{-1} from experimental data acquired at 2000 and 4000 rpm, respectively. These values represent the peak current measured at 2000 or 4000 rpm normalized to each molecule of O_2 converted to water on a per-enzyme basis.[23] In our modeling procedures, we equated the quantity $k_2[O_2]$ to that of the net rate, an assignment that was supported by the observation that the k_2' term in the numerator of eq 2 is weighted by a factor of f, resulting in a current density that scales almost entirely as a function of $k_2[O_2]$. As a result, the approximation $j \propto (k_2[O_2] - k_2'f) \approx k_2[O_2]$ holds under conditions relevant to catalysis. A value of 350 s^{-1} was assigned to k_3 based on previous measurements of formation of the native intermediate in laccases.[26] We set k_2' and k_3' to zero, as, to our knowledge, there exist no reports for the back-conversion of the peroxy intermediate to form the reduced enzyme, nor the native intermediate to the peroxy intermediate.

Using these values as inputs to the model gave a calculated LSV that agreed well with experimental data, accounting for properties of the electrochemical waves in both the low-overpotential (BV) and high-overpotential (O_2 diffusion-controlled) limits (Figure 2a). Overpotentials are referenced relative to the type 1 redox potential of laccase (~340 mV vs AglAgCl on ketjen black).[23] Allowing for a small variance in the calculated H_{AB} value (H_{AB} = 3.7 × 10^{-27} J, 190 μcm^{-1}), our model reproduced experimental data with minimized residuals. The switching point between the two catalytic regimes was evidenced by the change in concavity of the voltammogram between 0 and −250 mV overpotential. The point at which current goes from being controlled primarily by interfacial ET vs O_2 diffusion was therefore most apparent in the CV's derivative plot (Figure 2b). In this study, the quantity dj/dV took on a maximum value at about 110 mV overpotential, indicating catalysis was primarily controlled by interfacial kinetics below (and O_2 diffusion above) this value.

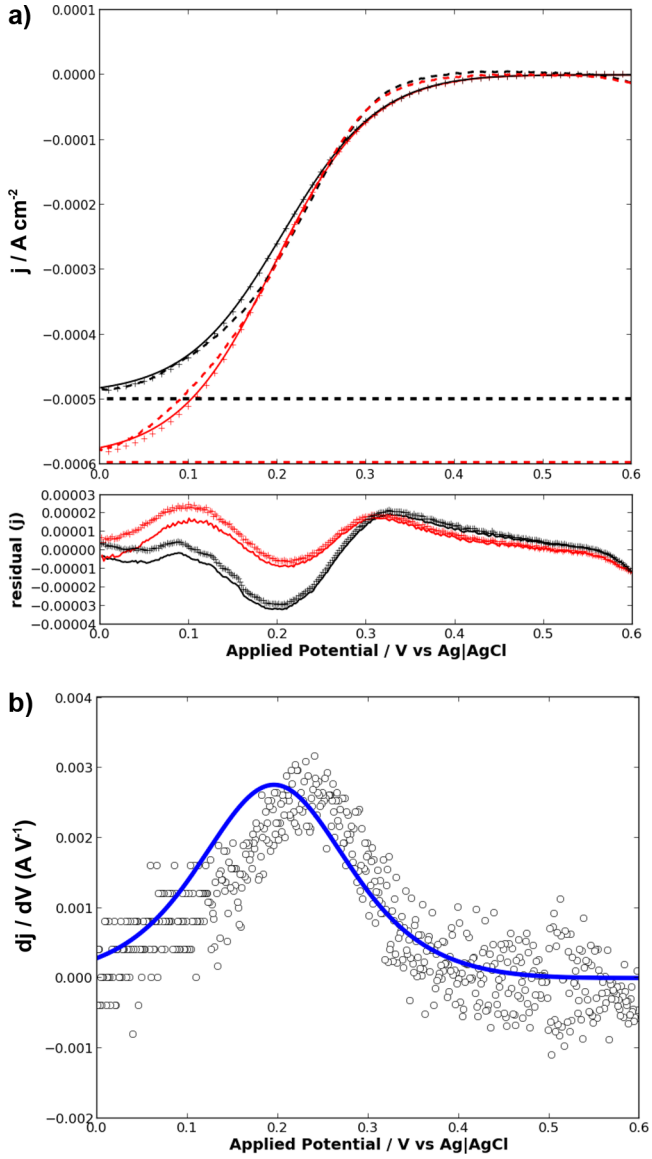

Figure 2. (a) J/V behavior for *Thermus thermophilus* strain HB27 laccase cathodes (black = 2000 rpm, red = 4000 rpm). Calculated voltammograms (solid lines) agree well with experimental data (−);[23] (+) markers denote the predictions of the rate law used by Kamitaka et al. The flat dotted lines represent the maximum current density for such electrodes as predicted by the high-overpotential limiting case of our MCO model (eq 7). The residual subplot indicates the difference between experimentally determined and modeled LSVs using our model (lines) and the rate law empoyed by Kamitaka (+). (b) Numerical differentiation of eq 2 yields a modeled differential voltammogram (blue line) that agrees well with experimental derivative LSV data (white dots). Conditions of electrode rotation at 2000 rpm ($k_2[O_2]$ = 5 s^{-1}) shown here. The derivative peaks highlight the region where current output is primarily controlled by interfacial kinetics (>230 mV vs AglAgCl) and mass transport of O_2(<230 mV).

Tafel plots generated using the model also gave promising results. The linear region of the modeled tafel trace extends for a much longer range of overpotentials than the linear region of the experimental data. However, the small overpotential region previously used for fitting tafel data had a slope (128 mV decade^{-1}) similar to that of the entire linear region of the modeled data (132 mV decade^{-1}), and the modeled exchange current (30.0 μA cm^{-2}) was close to the experimentally

dx.doi.org/10.1021/ja5077519 | J. Am. Chem. Soc. 2014, 136, 13882−13887

determined value (27.2 μA cm^{-2}).[23] The close agreement gave us confidence in the novel fitting methodology we employed previously, as it allowed for the identification of the proper region for conducting linear tafel analysis, despite the low-overpotential curvature that often obscures tafel fitting of data obtained from measurements on porous carbon MCO cathodes (Figure 3).[27]

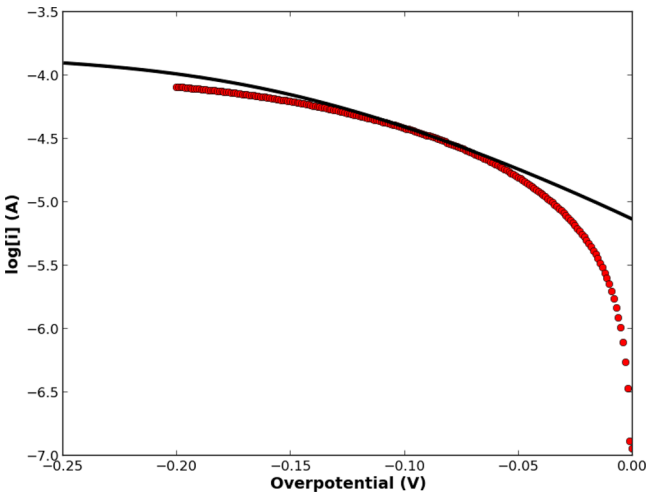

Figure 3. Tafel overlays of experimental[23] (red, circles) and modeled (black line) data. The −50 to −100 mV overpotential region previously used for fitting the data yielded a Tafel slope and exchange current that are similar to those obtained from the model.

DISCUSSION

Interfacial Charge-Transfer Rates. It is generally accepted in the field of protein electrochemistry that enzymes adsorb randomly onto porous carbon substrates, adopting configurations that position the active site at variable distances from the electrode.[4,19,28,29] As a result, experimental measurements of interfacial ET rates and electronic couplings represent values averaged over the broad range of surface orientations.

As we have determined the mean value of interfacial electronic coupling (H_{AB}) in laccase cathodes, we can estimate the average distance between the type 1 site and the electrode surface. Using the canonical driving-force optimized ($-\Delta G^0 = \lambda$) rate of 10^{13} s^{-1} for a donor−acceptor separation at closest contact (r_0),[30] we can express H^0_{AB} as follows:

$$H^0_{AB} = \frac{1}{2\pi} 10^{6.5} h^{0.5} (4\pi\lambda k_B T)^{0.25} \tag{9}$$

The average cathode-type 1 distance is then obtained from eq 10:

$$r = r_0 - \frac{2}{\beta} \ln \frac{H_{AB}(r)}{H^0_{AB}} \tag{10}$$

where β is the distance-decay constant. For the system under study, we find a value of 3.0 × 10^{-21} J (150 cm^{-1}) for the coupling at r_0 (3 Å). The average cathode-type 1 site separation falls in the range of 24−28 Å, assuming established β values of 1.3 and 1.1 A^{-1} for electron tunneling through α-helices and β-sheets.

Our finding of a 24−28 Å range for the average cathode-type 1 distance is also consistent with the work of Armstrong and co-workers, who demonstrated the utility of a uniform probability distribution function in accounting for rate dispersion in the interfacial charge-transfer kinetics of NiFe hydrogenase proton reduction cathodes.[29] In this approach, we may approximate the average distance between a type 1 acceptor and the electrode surface by using the expectation value of r:

$$\langle r \rangle = \int r P(r) dr \tag{11}$$

For a uniform distribution,

$$P(r) = \frac{1}{r_{max} - r_{min}} \tag{12}$$

It follows from eq 11 that the expectation value for a uniform distribution is simply the average of two distances:

$$\langle r \rangle = \frac{1}{2}(r_{max} + r_{min}) \tag{13}$$

.

Inspection of the laccase crystal structure (PDB: 2XU9) suggests that the closest distance between the type 1 site and the protein surface is approximately 10 Å, while the longest path is about 50 Å. From eq 13, we then obtain an average value of ca. 30 Å for the cathode-type 1 distance for randomly oriented enzymes. This result lies in close agreement with our value for the mean distance found using the value for H_{AB} derived from our kinetics model. Furthermore, the observed correspondence between these two methods for estimating the average donor−acceptor distance supports the long-held view that enzymes hydrophobically adsorbed on porous carbon substrates exhibit random surface orientations.

Adjusting our previously measured value of the interfacial ET rate (1.0 s^{-1} measured at $\Delta G^0 = 0$)[23] to its driving-force-optimized value of 16 s^{-1} enables direct comparison of the enzyme's electrochemical performance with known ET-distance relationships. We find that 16 s^{-1} electron tunneling over a distance of 25−30 Å places our system in a distance-decay region characteristic of beta-sheet proteins such as *Pseudomonas aeruginosa* azurin.[31] This result demonstrates a correlation between charge transport and protein secondary structure that conforms to known trends in macromolecular electron tunneling, despite the marked heterogeneity of the protein−electrode interface in these cathodes. As expected, these results also suggest an independence of tunneling behavior from the method used to determine ET rates, with our electrochemical data providing similar results to the photochemical methods that have been used to validate distance-decay relationships.[30,32−35]

Model Limitations and Features. We did not explicitly incorporate the complex problem of dioxygen flux through bulk solution in our model. As a result, the model is best suited for describing electrochemical behavior under conditions of nonlimiting dioxygen diffusion. It should be noted that experimental data used for model validation were acquired at 2000 rpm or higher, angular velocities where the rotational dependence of the catalytic current had essentially ceased.

We assumed that direct, interfacial charge transfer to the trinuclear cluster did not occur. This model of MCO catalysis, where the type 1 site acts as the initial point of reduction and relays charge to a trinuclear cluster that is heavily insulated from outer-sphere ETs by the peptide matrix, is generally accepted.[8,18,19,36−39]

dx.doi.org/10.1021/ja5077519 | J. Am. Chem. Soc. 2014, 136, 13882−13887

While in the derivation we allowed for reversibility in the transformation of the native intermediate in order to keep the model as general as possible ($k_4' \neq 0$), convincing arguments can be made for assigning this reverse interfacial rate constant a value near zero. A nonzero value for k_4' suggests that anodic ET, in concert with the rebinding of water at the MCO active site, is non-negligible, allowing for some degree of water oxidation at the trinuclear cluster. While such activity has been reported for *Trametes hirsuta* laccase,[40] the observed water oxidation occurred at potentials far more positive than those used in our modeling. As there is no evidence that these enzymes are capable of any oxidative chemistry at the low potentials we employed here, it is reasonable to assign k_4' a rate of 0 s^{-1}. In any case, these electrodes can only be operated cathodically, bracketing the maximum value of the anodic current to that of the exchange current, an already small value that quickly decays to zero as a cathodic bias is applied. As a result, modeling with k_4' set to zero gives similar output to that with k_4' made equal to the anodic term of the BV equation, with differences only becoming apparent at higher values of electronic coupling (Figure S.4).

As expected, enhanced electronic couplings between MCO type 1 sites and electrode surfaces are manifested by shallower tafel slopes and higher exchange current densities. However, the model suggests that for heterogeneous MCO cathodes fabricated with porous carbon substrates, increasing the electronic coupling beyond 10 H_{AB} (>3.7 × 10^{-26} J) will not result in appreciable reductions in the activation overpotential (Figure S.3). Furthermore, the optimization of peak catalytic currents by improving O_2 delivery also will suffer from the problem of successive enhancements becoming more difficult as a result of an expanding $k_2[O_2]$ term in the denominator of the rate expression.

CONCLUSIONS

We have developed a quantitative model for the electrochemical behavior of multicopper oxidases when functioning as heterogeneous catalysts. Notably, the model accounts for experimental data obtained from studies on *Thermus thermophilus* laccase cathodes.

We demonstrated that the predictive power of our model allowed for determination of cathode-type 1 electronic couplings and distance dispersions in laccase−surface interactions. Our work represents an advancement in understanding biological charge transport in heterogeneous electrochemical systems that should aid in the design of more efficient MCO cathodes.

ASSOCIATED CONTENT

Supporting Information

Annotated derivation of the rate law presented in this manuscript, additional figures demonstrating model predictions and thermal voltammetric data used for determination of type 1 copper reorganization energies and reductive titrations for determination of the type 1 redox potential in laccase. This material is available free of charge via the Internet at http://pubs.acs.org.

AUTHOR INFORMATION

Corresponding Author

hbgray@caltech.edu

Notes

The authors declare no competing financial interest.

ACKNOWLEDGMENTS

We thank Fan Liu, Joseph Varghese, and Jay Winkler for helpful discussions and the Beckman Institute Molecular Materials Research Center for access to equipment. This research was funded by the NSF CCI Solar Fuels Program (CHE-1305124) and a Perkins Grant (JRH.PERKINS3-1-GRANT.PERKINS3).

REFERENCES

(1) Miura, Y.; Tsujimura, S.; Kurose, S.; Kamitaka, Y.; Kataoka, K.; Sakurai, T.; Kano, K. *Fuel Cells* **2009**, *9*, 70−78.
(2) Liu, X.; Gillespie, M.; Ozel, A. D.; Dikici, E.; Daunert, S.; Bachas, L. G. *Anal. Bioanal. Chem.* **2011**, *399*, 361−366.
(3) Tsujimura, S. *Electrochim. Acta* **2008**, *53*, 5716.
(4) Cracknell, J. A.; Vincent, K. A.; Armstrong, F. A. *Chem. Rev.* **2008**, *108*, 2439−2461.
(5) Blanford, C. F.; Heath, R. S.; Armstrong, F. A. *Chem. Commun.* **2007**, 1710−1712.
(6) Lee, S.-K.; George, S. D.; Antholine, W. E.; Hedman, B.; Hodgson, K. O.; Solomon, E. I. *J. Am. Chem. Soc.* **2002**, *124*, 6180−6193.
(7) Lau, C.; Adkins, E. R.; Ramasamy, R. P.; Luckarift, H. R.; Johnson, G. R.; Atanassov, P. *Adv. Energy Mater.* **2012**, *2*, 162−168.
(8) Solomon, E. I.; Sundaram, U. M.; Machonkin, T. E. *Chem. Rev.* **1996**, *96*, 2563−2606.
(9) Sakurai, T.; Kataoka, K. *Chem. Rec.* **2007**, *7*, 220−229.
(10) Palmer, A. E.; Lee, S. K.; Solomon, E. I. *J. Am. Chem. Soc.* **2001**, *123*, 6591−6599.
(11) Sakurai, T.; Kataoka, K. *Cell. Mol. Life Sci.* **2007**, *64*, 2642−2656.
(12) Augustine, A. J.; Kjaergaard, C.; Qayyum, M.; Ziegler, L.; Kosman, D. J.; Hodgson, K. O.; Hedman, B.; Solomon, E. I. *J. Am. Chem. Soc.* **2010**, *132*, 6057−6067.
(13) Roberts, S. A.; Weichsel, A.; Grass, G.; Thakali, K.; Hazzard, J. T.; Tollin, G.; Rensing, C.; Montfort, W. R. *Proc. Natl. Acad. Sci. U. S. A.* **2002**, *99*, 2766−2771.
(14) Soukharev, V.; Mano, N.; Heller, A. *J. Am. Chem. Soc.* **2004**, *126*, 8368−8369.
(15) Miura, Y.; Tsujimura, S.; Kamitaka, Y.; Kurose, S.; Kataoka, K.; Sakurai, T.; Kano, K. *Chem. Lett.* **2007**, *36*, 132−133.
(16) Hong, G.; Ivnitski, D. M.; Johnson, G. R.; Atanassov, P.; Pachter, R. *J. Am. Chem. Soc.* **2011**, *133*, 4802−4809.
(17) Shleev, S.; Wang, Y.; Gorbacheva, M.; Christenson, A.; Haltrich, D.; Ludwig, R.; Ruzgas, T.; Gorton, L. *Electroanalysis* **2008**, *20*, 963−969.
(18) Kamitaka, Y.; Tsujimura, S.; Kataoka, K.; Sakurai, T.; Ikeda, T.; Kano, K. *J. Electroanal. Chem.* **2007**, *601*, 119−124.
(19) Blanford, C. F.; Foster, C. E.; Heath, R. S.; Armstrong, F. A. *Faraday Discuss.* **2008**, *140*, 319−335.
(20) Scodeller, P.; Carballo, R.; Szamocki, R.; Levin, L.; Forchiassin, F.; Calvo, E. J. *J. Am. Chem. Soc.* **2010**, *132*, 11132−11140.
(21) Bard, A. J.; Faulkner, L. R. *Electrochemical Methods: Fundamentals and Applications*, 2nd ed.; Wiley: New York, 2001.
(22) Bockris, J. O.; Reddy, A. K. N.; Gamboa-Aldeco, M. *Modern Electrochemistry 2A*, 2nd ed.; ; Springer: New York, 2000.
(23) Agbo, P.; Heath, J. R.; Gray, H. B. *J. Phys. Chem. B* **2013**, *117*, 527−534.
(24) Marcus, R. A.; Sutin, N. *Biochim. Biophys. Acta, Bioenerg.* **1985**, *811*, 265−322.
(25) Khoshtariya, D. E.; Dolidze, T. D.; Shushanyan, M.; Davis, K. L.; Waldeck, D. H.; Eldik, R.; van. *Proc. Natl. Acad. Sci. U. S. A.* **2010**, *107*, 2757−2762.
(26) Solomon, E. I.; Augustine, A. J.; Yoon, J. *Dalton Trans.* **2008**, 3921−3932.

(27) Thorum, M. S.; Anderson, C. A.; Hatch, J. J.; Campbell, A. S.; Marshall, N. M.; Zimmerman, S. C.; Lu, Y.; Gewirth, A. A. *J. Phys. Chem. Lett.* **2010**, *1*, 2251−2254.
(28) Armstrong, F. A.; Hill, H. A. O.; Oliver, B. N.; Walton, N. J. *J. Am. Chem. Soc.* **1984**, *106*, 921−923.
(29) Léger, C.; Jones, A. K.; Albracht, S. P. J.; Armstrong, F. A. *J. Phys. Chem. B* **2002**, *106*, 13058−13063.
(30) Gray, H. B.; Winkler, J. R. *Proc. Natl. Acad. Sci. U. S. A.* **2005**, *102*, 3534−3539.
(31) Gray, H. B.; Winkler, J. R. *Q. Rev. Biophys.* **2003**, *36*, 341−372.
(32) Lancaster, K. M.; Farver, O.; Wherland, S.; Crane, E. J.; Richards, J. H.; Pecht, I.; Gray, H. B. *J. Am. Chem. Soc.* **2011**, *133*, 4865−4873.
(33) Crane, B. R.; Di Bilio, A. J.; Winkler, J. R.; Gray, H. B. *J. Am. Chem. Soc.* **2001**, *123*, 11623−11631.
(34) Shih, C.; Museth, A. K.; Abrahamsson, M.; Blanco-Rodriguez, A. M.; Bilio, A. J. D.; Sudhamsu, J.; Crane, B. R.; Ronayne, K. L.; Towrie, M.; Vlček, A.; Richards, J. H.; Winkler, J. R.; Gray, H. B. *Science* **2008**, *320*, 1760−1762.
(35) Gray, H. B.; Winkler, J. R. *Biochim. Biophys. Acta, Bioenerg.* **2010**, *1797*, 1563−1572.
(36) Djoko, K. Y.; Chong, L. X.; Wedd, A. G.; Xiao, Z. *J. Am. Chem. Soc.* **2010**, *132*, 2005−2015.
(37) Kataoka, K.; Hirota, S.; Maeda, Y.; Kogi, H.; Shinohara, N.; Sekimoto, M.; Sakurai, T. *Biochemistry (Moscow)* **2011**, *50*, 558−565.
(38) Santos, L. dos; Climent, V.; Blanford, C. F.; Armstrong, F. A. *Phys. Chem. Chem. Phys.* **2010**, *12*, 13962−13974.
(39) Roberts, S. A.; Wildner, G. F.; Grass, G.; Weichsel, A.; Ambrus, A.; Rensing, C.; Montfort, W. R. *J. Biol. Chem.* **2003**, *278*, 31958−31963.
(40) Pita, M.; Mate, D. M.; Gonzalez-Perez, D.; Shleev, S.; Fernandez, V. M.; Alcalde, M.; De Lacey, A. L. *J. Am. Chem. Soc.* **2014**, *136*, 5892−5895.